Photocatalytic Removal of Amaranth Optimization Using Response Surface Methodology

Saeideh Ebrahimiasl[a,b,*], Ali Noori[b], and Azmi Zakria[c]

[a]Industrial Nanotechnology Research Center, Islamic Azad University, Tabriz, Iran
[b]Department of Chemical Engineering, Ahar Branch, Islamic Azad University, Ahar, Iran
[c]Department of Physic, University Putra Malaysia, Serdang, Malaysia

[*]Corresponding Author's Email: Ebrahimi.asl@iaut.ac.ir

ABSTRACT— Since Amaranth (AM) is one of the dye compounds which is harmful to human's life its removal from industrial waste water would reduce their environmental impact and health effect. Copper nanoparticle (CuNP) is a simple and eco-friendly material which can be used to remove this pollutant. In this paper, copper nanoparticles were synthesized, for removal of AM dye. The experiments were designed by response surface methodology with a modified cubic model to predict the variables. To investigate variables and interaction between them analysis of variance was used with high F-value (1.44), low P-value (<0.0409), non-significant lack of fit, the determination coefficient of 0.898 and the adequate precision of 7.25. Experimental and predicted values of the response illustrated a good correlation. The optimum parameters catalyst amount (0.14 w/w%), initial concentration (7.38 mg/l), reaction time (47.75 s) and pH (2.83) for the highest removal percentage of (96.10%) was attained.

KEYWORDS: Amaranth, Copper nanoparticles, Optimization, Photodegradation, Response surface methodology

I. INTRODUCTION

Photocatalytic degradation of pollution from surface and underground waters by different nanostructures is growing during past decade. The main parts of these pollutants are toxic materials which absorb on the surface of nanostructures and degrade during phototropy [1-2]. Photocatalysis is now the preferred method and has been successfully used to remove various types of coloring material such as activated carbon and biological treatment [3, 4]. Complete mineralization of pollutants, no requirement for disposal of sludge, and low energy consumption are advantages of this method.

AM is a well-known azo dye, which is widely used in textile mills, wood industry, paper-making industry and leathers for coloring. For quite long time it was also used as coloring agent for food stuff like jams, jellies, ketchup and cake decoration without attention to its carcinogenicity and other toxic effects. In the human being, prolong intake of AM can result to tumors, allergy, respiratory problems and birth defects [5-8]. Good solubility of AM in water is difficulties of its removal by common chemical treatments or by physical treatments like coagulation, froths floatation etc.

In the voluminous amount of research on photo-catalytic oxidation processes, titanium (IV) dioxide (TiO_2), iron and ZnO is the most widely used catalyst [9-11]. Toxic side effects of using this nanomaterial reduced its consumer confidence in water. Copper is one of the metals that have been a part of civilization for thousands of years. One of copper's more recent applications includes its use in food packaging [12] frequently touched surfaces (include frying pans, knives, forks and spoons), where copper's antimicrobial properties reduce the transfer of germs and disease. Copper is an essential nutrient to all

higher plants and animal life which is present in tissues, liver, muscles and bone. It acts as a co-factor in various enzymes and copper based pigments in the body. CuNPs with antimicrobial activity are new features of copper, issued against different microorganism (SCI Finder Scholar™, American Chemical Society) with expected higher disinfecting effects in nano scales [13-14].

The objective of this work is to use eco-friendly CuNPs for the photodegradation of AM from wastewaters. For this purpose, CN was synthesized using simple, low cost borohydrate reduction method. The synthesized CN under anaerobic conditions used for phototropy of an azo dyes (AM) that resulted in the cleavage of azo link in the dye molecule.

The dependence of the photo-oxidation rate on various parameters viz. initial dye concentration, catalyst dose, pH and electron acceptor concentration was investigated by multivariate optimization method which has more advantages over one-variable-at-a-time method. Study the interactive effects among the variables, minimum number of experiments and lower time and cost are the main parameters [15-16]. In response surface methodology, behavior of a data set describe by polynomial equation. In this method, the objective is the simultaneous optimization of the levels of variables [16]. In this study, the central composite rotatable design optimization was used for AM dye reduction by CN system. The effect of several parameters such as the catalyst amount, pH of solution, the reaction time and the initial concentration on the removal process was optimized.

II. EXPERIMENTS

A. *Materials and Methods*

AM dye molecular formula ($C_2OH_{11}N_2Na_3O_{10}S_3$; Mol. Wt. 604.6), copper sulfate ($CuSO_4$, $6H_2O$), sodium hydroxide, HCl and NaOH were obtained from Merck. Deionized distilled water (DDW) was used as a solvent in all experiments. Sodium

hydroxide (NaOH) was used as reducing agent to produce CN in aqueous solution via the reduction of copper Cu(II) [17-19]. In this work, NaOH solution (0.3 M) was gradually dropped into a $CuSO_4$, $6H_2O$ solution (0.1 M) under continues stirring. The copper ion (Cu^{2+}) was reduced to nano sized copper (Cu^0) precipitate as below:

$$2Cu^{+2} + 2OH^- + H_2O \rightarrow$$
$$2Cu^0 + 2H_2O + 1/2\,O_2 \tag{1}$$
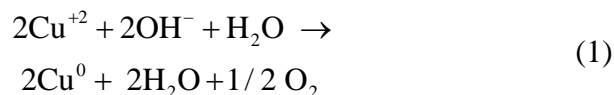
The molar ratio of substrates (NaOH: $CuSO_4+6H_2O$) was selected as 3:1 mole. The excessive sodium hydroxide (0.3 M) was applied to accelerate the synthesis reaction. The generated copper particles were filtered under vacuum, washed by DDW and dry in 120ºC. The dry CN particles were then characterized for the structures and sizes. Image of freshly synthesized copper nanoparticles identified by Scanning Electron Microscopy (SEM) (LEO-1455VP, England), is shown in Fig. 1. It is observed that the copper particles are in the form of nano-spheres having diameters of <100 nm.
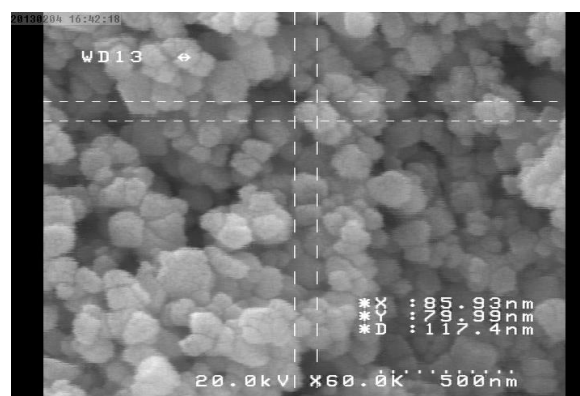

Fig. 1. Image of the prepared CuNPs by scanning electron microscopy (SEM).

XRD analysis was carried out with (Philips, PW3050) for prepared Cu^0 nanoparticles as shown in Fig. 2. The characteristic broad peak at 2θ of 43.751 is the characteristic peak of zero valent copper and indicate attendance of CN in the sample. An intense peak was observed for copper oxide in the XRD analysis. The observed copper oxide was
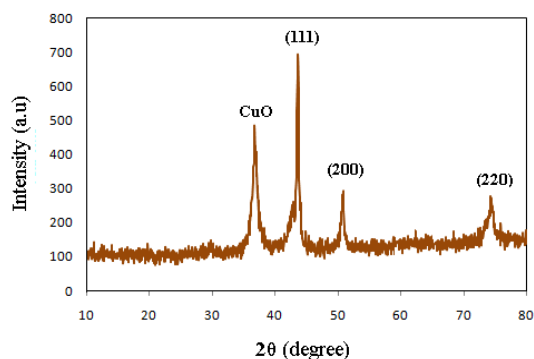
removed from the samples by heat treatment in 200 ℃.

Fig. 2. XRD pattern of synthesized copper nanoparticles

B. *Experimental Design*

The dye removal experiment was design by central composite design (CCD). The reaction time (s) (A), pH of solution (B), the initial concentration (mg/l) (C) and the catalyst amount (w/w %) (D), were center points in CCD, and used to evaluate the removal of AM dye. Experimental data were analyzed using (Design-Expert version 6.0.6) with a total of 30 experiments, including 16 factorial points (K2), 8 axial points (2K) and 6 central points (CP) [16].

Table 1 shows the design of experiment with four effective parameters for AM dye removal. Different mathematical models (linear, two factorial, quadratic and cubic) were used to design experiment of AM removal. The ANOVA of the models showed that the reaction of removal was most properly demonstrated with a ''quadratic'' polynomial model. The calculated F-value for each model is presented in Table 2. The topmost model with significant terms was chosen. The significance is assessed as the F-value calculated from the data exceeds a theoretical value [20]. The result of lack of fit test was evaluated for each sort of models and presented in Table 3. The models F-value was not significant for suggested models, thus manual modification of suggested models need to be conducted. To determine the extreme values of the variables, the preparatory experiments were done.

Table 1. Independent variables and their levels employed in the study

Variable	Unit	Limits					Step change value (ΔXi)
		-2	-1	0	1	2	
A-reaction time	min	30	40	50	60	70	10
B-pH	-	1	2	3	4	5	1
C-initial concentration	mol/dm^3	2	4	6	8	10	2
D-catalyst amount	(w/w%)	0.13	0.14	0.15	0.16	0.17	0.01

Table 2. Statistical parameters for sequential models

Source	Sum of squares	DF	Mean square	F value	Prob>F	Remarks
Mean	1.817E+005	1	1.817E+005	-	-	Suggested
Linear	3498.37	4	874.59	1.14	0.3596	Suggested
2F1	1727.04	6	287.84	0.31	0.9217	-
Quadratic	1605.48	4	401.37	0.38	0.8189	-
Cubic	8692.03	8	1086.50	1.07	0.4716	Aliased
Residual	7116.69	7	1016.67	-	-	-
Total	2.044E+005	30	6811.78	-	-	-

Table 3. Lack of fit tests result for sequential models

Source	Sum of squares	DF	Mean square	F value	Prob>F	Remarks
Linear	12597.23	20	629.86	0.48	0.8892	Suggested
2FI	10870.19	14	776.44	0.59	0.7973	
Quadratic	9264.71	10	926.47	0.71	0.7004	
Cubic	572.67	2	286.34	0.22	0.8108	Aliased
Pure Error	6544.02	5	1308.80			

III. RESULTS AND DISCUSSION

A. *Analysis of the Model*

The predicted values versus actual values are shown in Fig. 3. The predicted responses obtained from RSM shows a good overlap to the actual responses and verify the predicted data. The root mean squares error (average of the square of all of the error) (RMSE = 2.657) calculated for the model, demonstrated minimum differences between actual and predicted values. The coefficient of determination (R^2= 0.898) and the relative standard deviation (RSD = 3.414) determined for the model, indicates well data fit to statistical model. The RSD are calculated by the following equations:

$$Cv = \frac{\sigma}{\mu} \qquad (2)$$

where μ is the mean and σ is standard deviation [21]. The adjusted determination coefficient (adjusted R^2=0.813) was also indicates that the model is a good fit for the data.

The normality of the observations was examined by the normal possibility diagram of residuals. In the normal distribution of errors, the normality diagram is straight line.
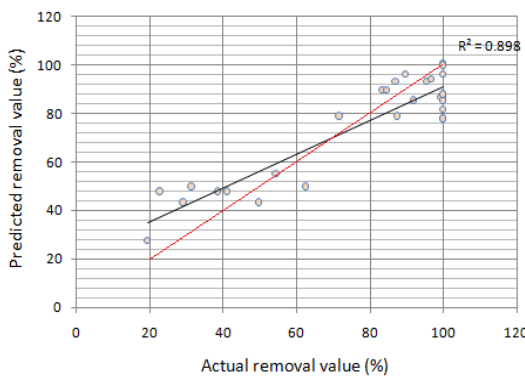

Fig. 3. Scatter plot of predicted value of removal (%) versus actual value of removal (%) from the RSM design.

Residuals coordination is presented in Fig. 4 (A). If the correct model and hypotheses were fulfilled, the residuals must independently distributed with run numbers and without

special relation to the other variables like the predicted response. The result reveals independently distribution of residuals with run numbers and accordingly, priority of the chosen model.
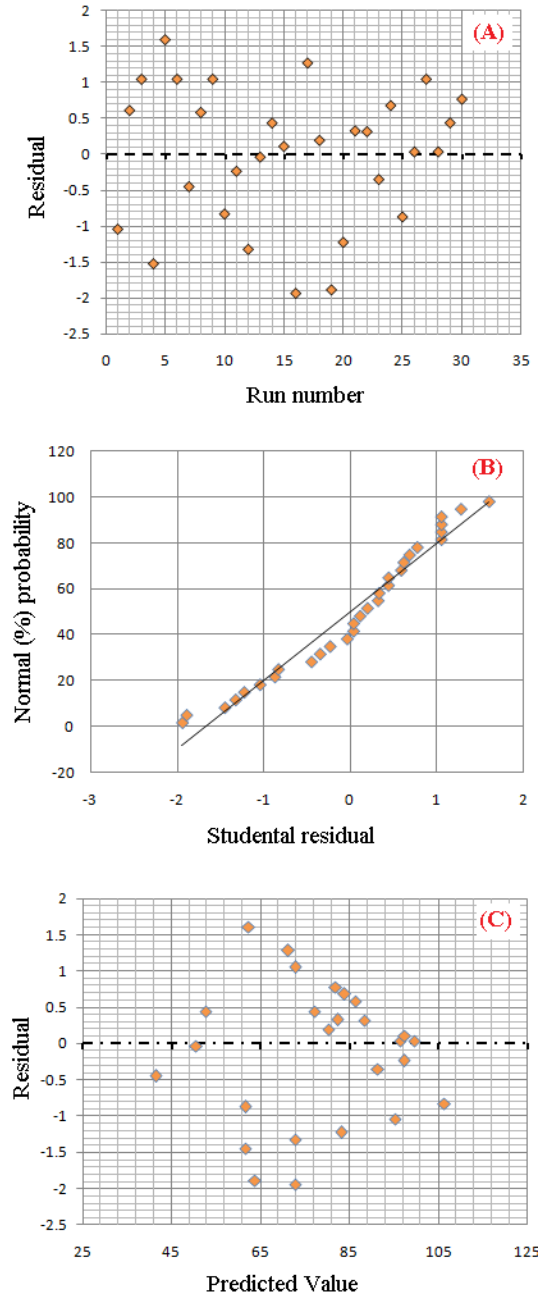

Fig. 4. Residual plots for dye reduction efficiency by (a) chronological diagram of the residuals, (b) diagram of the residuals based on the predicted amounts of degradation percent efficiency, (c) residuals normal possibility diagram.

Figure 4 (B) shows the residuals normal possibility diagram. Normality of observation appears in the normal probability diagram of

residuals. The straight line in the resulting diagram indicated normal distribution of residuals. Therefore, as it reveals from the diagram, the distribution of the faults is pretty normal. The diagram of the residuals versus on the corresponding predicted amounts of degradation efficiency are presented in Fig. 4(C). As it is reveals, residuals versus fitted values plot do not show increasing residuals and produce a randomly distribution of scattered points.

The ANOVA results of the modified linear model for the AM photodegradation are presented in Tables 4. The ANOVA depict any significant differences between the means of independent (unrelated) variables. The amount of F-value has been calculated for each model. A larger F-value is better to find a significant effect and indicate a consistent pattern is unlikely due to chance. The more the amount of F-value goes, the less the amount of P-value gets. P-value less than 0.05, demonstrated that, purposed factor is meaningful. F-value of 1.44 indicates that the model was significant. The amount of critical F-value is calculated according to the equation ($F_{0.05,df,(n-df+1)}$), since ($F_{0.05,14,15} = 2.42$) is lower than the calculated F-value, the model is meaningful (Table 4) [22-23].

The coefficient of determination (R^2) of the model should be between zero and one. The larger amount of R^2 indicated variability in the response conveniently could be explained by the model. Therefore, the present R^2-values (0.898) reflected a very good fit between the experimental and predicted values [24].

The adjusted R^2 always lower than the R-squared and compares the explanatory power of regression models that contain different numbers of predictors. The adjusted R^2 (0.813) for this model was satisfactory, which confirms the fitness of the model [25]. The adequate precision (7.426) shows remarkable signal (>>4) and depicted that suggested model was suitable to navigate the design space. Thus it provides a satisfactory match of the polynomial model to the experimental data. Morever, the "Lack of Fit F-value" of 0.40 implies the Lack of Fit is not significant relative to the pure error. Non-significant lack of fit indicates that the model is fit.

Table 4. Analysis of variance (ANOVA) of the response surface linear model for the prediction of dye reduction efficiency.

Source	Sum of squares	DF	Mean of square	F value	Prob>F	
Model	7103.84	7	1014.83	1.44	0.0409	Significant
A	652.24	1	652.24	0.92	0.03470	
B	491.51	1	491.51	0.70	0.04131	
C	2353.91	1	2353.91	3.33	0.00815	
D	746.09	1	746.09	1.06	0.03152	
C^2	1148.49	1	1148.49	1.63	0.02155	
AC	1492.16	1	1492.16	2.11	0.01602	
C^3	964.82	1	964.82	1.37	0.02550	
Residual	15535.78	22	706.17			
Lack of fit	8991.76	17	528.93	0.40	0.9263	Not significant
Pure error	6544.02	5	1308.80			
Cor total	22639.62	29				
Std. Dev.		2.657		R-squared		0.898
Mean		77.83		Adj-R-squared		0.813
C.V.		34.14		Pred R-squared		0.680
PRESS		2327.356		Adeq precision		4.726

Table **5.** Response surface central composite design for predicted and experimental response

Run no.	Reaction time (min)	pH	Initial concentration (mg/l)	Catalyst amount (w/w%)	Actual removal (%)	Predicted removal (%)
1	-1	-1	1	1	71.6216	61.65
2	-1	1	1	1	99.9	91.39
3	0	0	0	0	99.9	52.60
4	-1	-1	-1	-1	28.9926	82.34
5	-2	0	0	0	99.9	106.31
6	0	0	0	0	99.9	97.42
7	-1	1	-1	1	31.2807	97.25
8	1	-1	1	1	99.4186	88.37
9	0	0	0	0	99.9	50.50
10	-1	-1	1	-1	87.5675	80.24
11	-1	1	1	-1	91.9254	41.45
12	0	0	0	0	38.4615	71.19
13	-1	-1	-1	1	49.624	95.15
14	1	1	1	1	87.027	86.27
15	1	-1	1	-1	99.9	86.10
16	0	0	0	0	22.5806	77.22
17	1	1	-1	1	99.9	62.35
18	1	-1	-1	1	84.6153	83.20
19	0	2	0	0	19.3181	81.83
20	2	0	0	0	54.364	63.72
21	1	1	-1	-1	89.7435	99.60
22	1	1	1	-1	95.5056	96.48
23	1	-1	-1	-1	83.489	83.93
24	0	0	0	-2	99.9	61.62
25	0	0	0	2	41.1111	72.78
26	0	0	-2	0	99.9	72.78
27	0	0	0	0	99.9	72.78
28	0	0	2	0	96.7799	72.78
29	-1	1	-1	-1	62.5	72.78
30	0	-2	0	0	99.9	72.78

Table 5 show the empirical results of AM dye degradation by nano copper and the matrix of four variable central composite design. For relating independent variables to dependent ones, the polynomial response quadratic has been used. The result reveals an empirical relation between independent variables and the response. This relation is presented in the following third-order polynomial equation:

$$Y = +125.48803 + 3.41845A - 4.52543B - 46.75055C - 557.55917D + 11.66628C^2 - 0.48286AC - 0.56042C^3 \tag{2}$$

The efficiency of AM degradation predicted by Eq. (3), is presented in Table 5.

A high conformity between the amounts of empirical removal efficiency and the predicted one was observed.

B. *Response Surface Plots*

The three dimensional plots in Fig. 5 is presented the numerous simulated responses with the four variables and one response of the photodegradation of AM dye based on the validated model.

The interactions between two tested variables on the degradation efficiency are presented at fixed levels of all other variables. The effect of pH, reaction time, initial concentration and catalyst amount on photodegradation of AM dye was investigated during the photodegradation as a preliminary study. Three-dimensional response surface plots were

organized based on the quadratic model with the optimum level of the relative variables in the central point in the upmost level in each of these figures.

Mutual interaction of pH (1-5) and reaction time (30-70) with constant catalyst amount (0.15 w/w %) and initial concentration (6 mol/dm^3) of AM dye are presented in Fig. 5A.

In a low pH, copper has the positive surface charge due to H+ concentration increase in the solution and adsorbs the compounds with the negative charges like anionic dyes. When the pH of solution increase, the copper surface gets the negative charge due to the presence of OH$^-$ in the solution and can make a complex with cationic compounds. So, according to these considerations, the acidic conditions are more ideal for AM dye photodegradation, as while as, AM is an anionic and acidic dye.

The impact of the AM dye initial concentration (10–50 mg/l) and reaction time (30-70) on the photodegradation efficiency in the fixed amounts of catalyst (0.15 w/w%) and pH (3) is shown in Fig. 5B. This diagram shows that the efficiency of photodegradation increases as the dye initial concentration increases and that is argue for increase in the number of molecules stick to CN surface and remove from the solution. However, there are not enough spaces for all molecules in high concentration of dye.

Mutual interaction of the dye initial concentration and pH on the photodegradation efficiency in the fixed amount of catalyst (0.15 w/w%) and reaction time (50 min) is observed in Fig. 5C. It clearly states that as the pH increases, the photodegradation efficiency decrease for different concentration of AM dye. In acidic pH, more H+ exists in the solution and react with different concentration of AM dye molecules abandon its concentration.

The mutual interaction of variables reveals that pH of the solution and AM dye concentration, are more effective on photodegradation of AM efficiency than other variables. The influence

of catalyst amount and time on the efficiency of AM dye photodegradation is negligible.
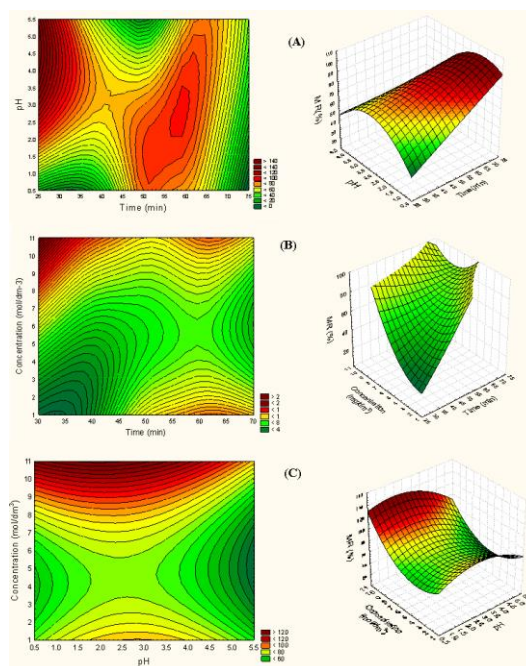
Fig. 5. The response surface and counter plots showing effect of (a) reaction time and pH, (b) initial concentration and reaction time, (c) pH of solution and initial concentration on dye reduction by the CuNPs.

C. *Model Validation*

To predict the optimum conditions for AM dye photodegradation by nano copper three solutions with different amounts of ideal conditions were purposed. Experiments were done under fixed condition and the obtained response values were compared to the predicted amounts. The highest percent of removal (96.102) was gained in the experiment number 3, among all experiments. Optimum parameters of the reaction was obtained by this experiment: catalyst amount (0.14 w/w%), initial concentration (7.38 mg/l), reaction time (47.75 s) and pH (2.83). The relative deviation coefficient 2.12% was gained from RSM experimental design. The comparison between actual and predicted amounts shows a good relation.

IV. CONCLUSION

The photodegradation of AM dye by CuNPs was optimized using RSM. A central composite design was applied to provide the

experimental conditions for removing the dye. Four effective factors including catalyst amount, pH of solution, reaction time and initial concentration were chose to design the experiments. The responses were fitted with a quadratic model to suggest a model for photodegradation among all the models. The ANOVA result, confirmed high validity of the model with the high F-value (1.44), non-significant lack of fit, the determination coefficient of $R^2 = 0.898$ and the adequate precision of 7.25. A removal percentage of 90.10% was attained by suggested optimum experimental condition, which has good compatibility to the predicted amount of 87.83%, with the relative deviation percentage of 2.12%. Thus, useful knowledge's were obtained for wastewater treatment by influences of CuNP on optimizing the potential parameters of AM dye degradation.

REFERENCES

[1] T. Havuz, B. Dönmez, and C. Çelik, "Optimization of removal of lead from bearing-lead anode slime," Ind. Eng. Chem. Res. Vol. 16, pp. 355-363, 2010.

[2] M. Sohrabi and M. Ghavami, "Comparison of Direct Yellow 12 dye degradation efficiency using UV/semiconductor and UV/H 2 O 2/semiconductor systems," Desalination, Vol. 252, pp. 157-162, 2010.

[3] M. Karkmaz, E. Puzenat, C. Guillard, and J. Herrmann, "Photocatalytic degradation of the alimentary azo dye amaranth: Mineralization of the azo group to nitrogen," Appl. Catal. B Environ, Vol. 51, pp. 183-194, 2004.

[4] C.-H. Wu, "Comparison of azo dye degradation efficiency using UV/single semiconductor and UV/coupled semiconductor systems," Chemosphere, Vol. 57, pp. 601-608, 2004.

[5] R.A. Simon, "Adverse reactions to drug additives," J. Allergy Clin. Immunol, Vol. 74, pp. 623-630, 1984.

[6] J.A. Bantle, D.J. Fort, J.R. Rayburn, D.J. Deyoung, and S.J. Bush, "Further validation of FETAX: evaluation of the developmental toxicity of five known mammalian teratogens and non-teratogens," Drug Chem. Toxicol. Vol. 13, pp. 267-282, 1990.

[7] V.K. Gupta, R. Jain, A. Mittal, T.A. Saleh, A. Nayak, S. Agarwal, Sh. Sikarwarc, "Photo-catalytic degradation of toxic dye amaranth on TiO 2/UV in aqueous suspensions," Mater. Sci. Eng. C, Vol. 32, pp.12-7, 2012.

[8] M.M. Hashem, A.H. Atta, M.S. Arbid, S.A. Nada, and G.F. Asaad, "Immunological studies on Amaranth, Sunset Yellow and Curcumin as food colouring agents in albino rats," Food Chem. Toxicol, Vol. 48, pp. 1581-1586, 2010.

[9] M. Faisal, A.A. Ismail, A.A. Ibrahim, H. Bouzid, and S.A. Al-Sayari, "Highly efficient photocatalyst based on Ce doped ZnO nanorods: Controllable synthesis and enhanced photocatalytic activity," Chem. Eng. J. Vol. 229, pp. 225-33, 2013.

[10] R.M. Alberici and W.F. Jardim, "Photocatalytic destruction of VOCs in the gas-phase using titanium dioxide," Appl. Catal. B Environ, Vol. 14, pp. 55-68, 1997.

[11] H. Hidaka, J. Zhao, E. Pelizzetti, and N. Serpone, "Photodegradation of surfactants. 8. Comparison of photocatalytic processes between anionic DBS and cationic BDDAC on the titania surface," J. Phys. Chem. A, Vol. 96, pp. 2226-2230, 1992.

[12] S. Ebrahimiasl and A. Rajabpour, "Synthesis and characterization of novel bactericidal Cu/HPMC BNCs using chemical reduction method for food packaging," J. Food Sci. Technol, Vol. 22, pp. 1-7, 2014.

[13] G. Faúndez, M. Troncoso, P. Navarrete, and G. Figueroa, "Antimicrobial activity of copper surfaces against suspensions of Salmonella enterica and Campylobacter jejuni," BMC Microbiology, Vol. 4, pp. 19-30, 2004.

[14] M. Valodkar, P.S. Rathore, R.N. Jadeja, M. Thounaojam, R.V. Devkar, and S. Thakore, "Cytotoxicity evaluation and antimicrobial studies of starch capped water soluble copper nanoparticles," J. Hazard. Mater. Vol. 201, pp. 244-249, 2012.

[15] M. Sohrabi and M. Ghavami, "Photocatalytic degradation of Direct Red 23 dye using UV/TiO 2: Effect of operational parameters," J. Hazard. Mater. Vol. 153, pp. 1235-1239, 2008.

[16] M.A. Bezerra, R.E. Santelli, E.P. Oliveira, L.S. Villar, and L.A. Escaleira, "Response

surface methodology (RSM) as a tool for optimization in analytical chemistry," Talanta, Vol. 76, pp. 965-977, 2008.

[17] T. Masciangioli and W.-X. Zhang, "Peer reviewed: environmental technologies at the nanoscale," Environ. Sci. Technol, Vol. 37, pp. 102A-108A, 2003.

[18] L. Zhang, L. Zhang, and M. Wan, "Molybdic acid doped polyaniline micro/nanostructures via a self-assembly process," Eur. Polym. J. Vol. 44, pp. 2040-2045, 2008.

[19] X.-M. Miao, R. Yuan, Y.-Q. Chai, Y.-T. Shi, and Y.-Y. Yuan, "Direct electrocatalytic reduction of hydrogen peroxide based on Nafion and copper oxide nanoparticles modified Pt electrode," J. Electroanal. Chem, Vol. 612, pp. 157-163, 2008.

[20] R. Muralidhar, R. Chirumamila, R. Marchant, and P. Nigam, "A response surface approach for the comparison of lipase production by Candida cylindracea using two different carbon sources," Biochem. Eng. J. Vol. 9, pp. 17-23, 2001.

[21] P. Aleksandrov and A.-R. Slovar Matematicheskikh, "Dictionaries and Encyclopedias," Guide to Information Sources in Mathematics and Statistics, Vol. 79, 2004.

[22] R. Sen and T. Swaminathan, "Response surface modeling and optimization to elucidate and analyze the effects of inoculum age and size on surfactin production," Biochem. Eng. J. Vol. 21, pp. 141-148, 2004.

[23] K. Yetilmezsoy and A. Saral, "Stochastic modeling approaches based on neural network and linear–nonlinear regression techniques for the determination of single droplet collection efficiency of countercurrent spray towers," Environmental Modeling & Assessment, Vol. 12, pp. 13-26, 2007.

[24] Y. Li, J. Lu, G. GU, and Z. MAO, "Characterization of the enzymatic degradation of arabinoxylans in grist containing wheat malt using response surface methodology," J. Am. Chem. Soc, Vol. 63, pp. 171-176, 2005.

[25] S. Ebrahimiasl and A. Zakaria, "Simultaneous Optimization of Nanocrystalline SnO2 Thin Film Deposition Using Multiple Linear Regressions," Sensors, Vol. 14, pp. 2549-2560, 2014.

Saeideh Ebrahimiasl received her Ph.D in Nanomaterial and Nanotechnology, from Institute of Advanced Materials, University of Putra Malaysia in 2010.

She is now an associate professor and head of Industrial Nanotechnology Research Center, Islamic Azad University, Tabriz, Iran and also an academic member of Islamic Azad University, Ahar Branch, Ahar, Iran.

Professor Azmi Zakria was a professor of Applied Optics in the physics Department, Universiti Putra Malaysia (UPM), Malaysia.

He was born in 1954, received his M.Sc in Optoelectronics (1981) and Ph.D in Photothermal physics (1994) from UK universities. His areas of experience are photothermal physics and spectroscop, solar energy, zinc oxide based varistor and nanomaterials.

Ali Noori received his MS.c. in Chemical Engineering from Department of Engineering, Islamic Azad University in 2016.

THIS PAGE IS INTENTIONALLY LEFT BLANK.